NeuroImage: Clinical 25 (2020) 102139

Contents lists available at ScienceDirect

NeuroImage: Clinical

journal homepage: www.elsevier.com/locate/ynicl

Early alterations in cortical and cerebellar regional brain growth in Down Syndrome: An *in vivo* fetal and neonatal MRI assessment

Prachi A. Patkee[a], Ana A. Baburamani[a], Vanessa Kyriakopoulou[a], Alice Davidson[a], Elhaam Avini[a], Ralica Dimitrova[a,b], Joanna Allsop[a], Emer Hughes[a], Johanna Kangas[b], Grainne McAlonan[b], Mary A. Rutherford[a]

[a] Centre for the Developing Brain, School of Biomedical Engineering and Imaging Sciences, King's College London, St. Thomas's Hospital, London, SE1 7EH, United Kingdom
[b] Department of Forensic and Neurodevelopmental Science, Sackler Institute for Translational Neurodevelopment, Institute of Psychiatry, Psychology and Neuroscience, King's College London, SE5 8AB, United Kingdom

ARTICLE INFO

Keywords:
Brain
Down Syndrome
MRI
Fetal
Neonatal

ABSTRACT

Down Syndrome (DS) is the most frequent genetic cause of intellectual disability with a wide spectrum of neurodevelopmental outcomes. At present, the relationship between structural brain morphology and the spectrum of cognitive phenotypes in DS, is not well understood. This study aimed to quantify the development of the fetal and neonatal brain in DS participants, with and without a congenital cardiac defect compared with a control population using dedicated, optimised and motion-corrected *in vivo* magnetic resonance imaging (MRI). We detected deviations in development and altered regional brain growth in the fetus with DS from 21 weeks' gestation, when compared to age-matched controls. Reduced cerebellar volume was apparent in the second trimester with significant alteration in cortical growth becoming evident during the third trimester. Developmental abnormalities in the cortex and cerebellum are likely substrates for later neurocognitive impairment, and ongoing studies will allow us to confirm the role of antenatal MRI as an early biomarker for subsequent cognitive ability in DS. In the era of rapidly developing technologies, we believe that the results of this study will assist counselling for prospective parents.

Introduction

Down Syndrome (DS) is the most common genetic cause of intellectual disability, occurring as a result of triplication of a genomic region on human chromosome 21 (Trisomy 21; T21) (Holtzman, 1996; Antonarakis et al., 2004). The neurodevelopmental phenotype of DS is associated with cognitive deficits with varying degrees of impairment of speech, motor and language functions, with a wide and largely unexplained spectrum of IQ's (range = 20–80; mean = 50) (Määttä et al., 2006; Rachidi and Lopes, 2007; Bartesaghi et al., 2011; Karmiloff-Smith et al., 2016). Approximately 50% of DS babies are born with a congenital heart defect (CHD), the most common of which are endocardial cushion defects, including atrioventricular septal defects (AVSD; 45%) and ventricular septal defects (VSD; 35%) (Hyett et al., 1996; Roizen and Patterson, 2003; Sherman et al., 2007; Bergstrom et al., 2016). The presence of cardiac disease is associated with a poorer outcome, as observed in typically developing children with CHD, where studies have shown deficits in neurocognitive, motor and psychosocial skills (Razzaghi et al., 2015). Children with DS who have an AVSD have been shown to have poorer gross motor skills, cognition and lower scores in expressive and receptive vocabulary, as compared to DS children with a structurally normal heart (Visootsak et al., 2011, 2013, 2016). However, there is limited information regarding structural brain development in the presence or absence of a CHD in DS.

The severity and range of problems experienced in DS are determined, in part, by overexpression of specific genes on the extra chromosome, and dysregulation of their associated pathways (Rachidi and Lopes, 2011; Guedj et al., 2016). At present, there is little known about early brain growth trajectories in DS and the spectrum of cognitive phenotypes. Abnormalities in brain development in DS, such as reductions in cortical and cerebellar volumes, have been observed in early life predominantly through postmortem cases, but there is little *in vivo* information about when atypical brain growth and development patterns may emerge (Hamner et al., 2018). Ultrasound studies (US) have concentrated on first trimester findings to assist in early diagnosis (Borenstein et al., 2006), with a few small sampled studies focusing on the second and third trimester, and noting smaller head circumferences

E-mail address: mary.rutherford@kcl.ac.uk (M.A. Rutherford).

https://doi.org/10.1016/j.nicl.2019.102139
Received 27 June 2019; Received in revised form 15 December 2019; Accepted 21 December 2019
Available online 23 December 2019

and cerebellar diameters (Winter et al., 2000).

Previous studies have largely focused on children and adults with DS, which makes it difficult to untangle the primary pathophysiological and direct effects of the condition on the brain, from the secondary or compensatory mechanisms which arise from living with the disorder. To reduce these confounds, a more detailed understanding of early *in vivo* growth of the cortex and cerebellum, may allow us to identify early biomarkers to predict the severity of initial cognitive impairments, and improve counselling for prospective parents. It also has the potential to reveal new windows for future therapeutic intervention strategies aimed at improving neurodevelopmental outcomes.

The primary objective of this study was to use MR imaging techniques to investigate the developing brain across gestation, in a cohort of fetuses and neonates with DS, with and without a CHD. We aimed to objectively quantify three-dimensional (3D) volumetric and two-dimensional (2D) linear measurements of whole brain, cortex and cerebellum and to compare these with aged-matched control cases. We hypothesised that there are quantifiable alterations in early cortical and cerebellar growth in fetuses and neonates with DS as compared with controls and that these are further altered by the presence of a cardiac abnormality.

Methods

Ethical approval for this study was obtained from the West London and GTAC Research Ethics Committee (REC) for DS participants and fetal controls (07/H0707/105); and from the Dulwich NREC for neonatal controls (12/LO/2017). Informed consent was obtained from all participants or their legal guardians, prior to imaging at Hammersmith Hospital and St. Thomas' Hospital, London, UK. All methods were carried out in accordance with the relevant guidelines and regulations.

Participants

Pregnant women with a fetus diagnosed with DS or with a high risk for DS were referred from antenatal and fetal medicine clinics across London hospitals, following their anomaly scans, amniocentesis, or blood test results. Ex-fetal participants who consented during their initial scan to be contacted post-delivery, were invited for a neonatal scan up to 46 weeks post-menstrual age (PMA). Additionally, neonates with confirmed DS were recruited from the neonatal unit or postnatal wards at St Thomas' Hospital. Participants with DS and other non-brain congenital abnormalities such as CHDs or gastrointestinal malformations were also included in this study. The presence and characteristics of any antenatally detected CHD were confirmed on echocardiography postnatally as part of a routine clinical assessment. Clinical details for all fetuses and neonates with DS can be found in Supplementary Table 1. Cases with any overt malformations as detected on MRI were excluded.

Healthy pregnant volunteers were recruited from the antenatal clinics at Queen Charlotte's and Chelsea Hospital and St. Thomas' Hospital, London at the time of their anomaly scans (approximately 20 weeks' gestational age (GA)) or self-referred. The entry criterion for a low risk fetal control for this study, was a normal brain appearance as determined by fetal MRI and confirmed by an experienced perinatal neuroradiologist. Fetuses with other congenital or chromosomal abnormalities, women with a history of drug use, twin pregnancies, pregnancies with delivery complications resulting in neonatal neurological complications were excluded from the study. In addition, fetal participants with an abnormal appearance of the brain on neonatal MRI, birth weight below the 3rd centile, premature birth ($<$ 37 weeks GA), sub-optimal MR image quality and with an abnormal outcome at either the year 1 or 2 neurodevelopmental assessments were also excluded. Control group neonates were only recruited from South London and South East of England antenatal centres as part of the Brain Imaging in Babies Study (BIBS), and scanned at the Centre for the Developing Brain (St. Thomas' Hospital, London). Neonates were included based on a normal neonatal brain appearance on MRI, classified as having no structural anomalies and no clinically significant acquired findings, with no other congenital or chromosomal abnormalities, and a normal neurodevelopmental outcome at 2 years of age.

Fetal image acquisition

Fetal MRI was performed on a 1.5-Tesla (1.5T) or 3-Tesla (3T) MRI System (Philips Achieva; Philips Medical Systems, Best, The Netherlands) using a 32-channel cardiac array coil placed around the maternal abdomen. Participants were scanned in either left lateral or supine position and provided with a pregnancy pillow and foam wedges for comfort. Maternal temperature was taken before and after the scan, and maternal heart rate was monitored throughout. Sedatives were not administered and the total scan time was restricted to 60 min. All fetal control data was acquired on a 1.5T scanner; fetal DS patients were scanned on a combination of 1.5T (n = 12) and 3T scanners (n = 18).

Fetal T2-weighted images were acquired in the transverse, sagittal and coronal plane using single shot turbo spin echo (ssTSE) sequences with the following scanning parameters: repetition time (TR) = 15 s; echo time (TE) = 160 ms; slice thickness = 2.5 mm with a slice overlap = 1.5 mm; and flip angle = 90°. The brain was oversampled by acquiring multiple overlapping single shot T2-weighted images to ensure complete coverage of all regions of interest within the brain. The TR on the 1.5T and 3T scanners was determined by the B1 amplitude. The TE was the same on both scanners.

3D reconstructed images were obtained using Snapshot MRI with Volume Reconstruction (SVR) from 2D slices (Jiang et al., 2007; Kuklisova-Murgasova et al., 2012). A stack of images with the least motion and artefacts was selected as the target, and a mask was created to isolate the fetal brain from surrounding maternal and extracranial fetal tissue, using ITK-SNAP (version 2.4.0; Yushkevich et al. 2006) (Yushkevich et al., 2006). The optimised reconstruction algorithm used intensity matching to exclude mis-registered or corrupted voxels and slices. The approved slices were registered into a common coordinate space for alignment, to produce the resultant high signal-to-noise ratio images. The reconstructed brains were manually re-orientated and then resampled from 1.25 × 1.25 × 1.25 mm to a voxel size of 0.2 × 0.2 × 1 mm, to improve the resolution of smaller structures (Kyriakopoulou et al., 2017). The datasets provide complete coverage of the brain in the orthogonal planes, which is optimum for detailed volumetric analysis.

Neonatal image acquisition

Neonatal MR scanning was performed on a Philips Achieva 3-Tesla system (Best, The Netherlands) at the Centre for the Developing Brain (St. Thomas' Hospital, London) using a dedicated 32 channel neonatal head coil. Infants were placed and secured within the scanning shell and a neonatal positioning device was used to stabilise the head to reduce movement (Hughes et al., 2017). Auditory protection was comprised of earplugs moulded from silicone-based putty placed in the outer ear (President Putty, Coltene/Whaledent Inc., OH, USA), neonatal earmuffs over the ear (MiniMuffs, Natus Medical Inc., CA, USA) and an acoustic hood placed over the scanning shell. Sedation was not administered and all babies were scanned during natural sleep. Scan time was restricted to 60 min. An experienced neonatologist was present during the examinations and pulse oximetry, heart rate, and temperature were monitored throughout the scan.

T2-weighted images were acquired in the sagittal and transverse planes using a multi-slice turbo spin echo sequence. Two stacks of 2D slices were acquired using the scanning parameters: TR = 12 s; TE = 156 ms; slice thickness = 1.6 mm with a slice overlap = 0.8 mm; flip angle = 90° and an in-plane resolution: 0.8 × 0.8 mm.

Visual analysis of all fetal and neonatal images was performed by a specialist perinatal radiologist to exclude additional anomalies and

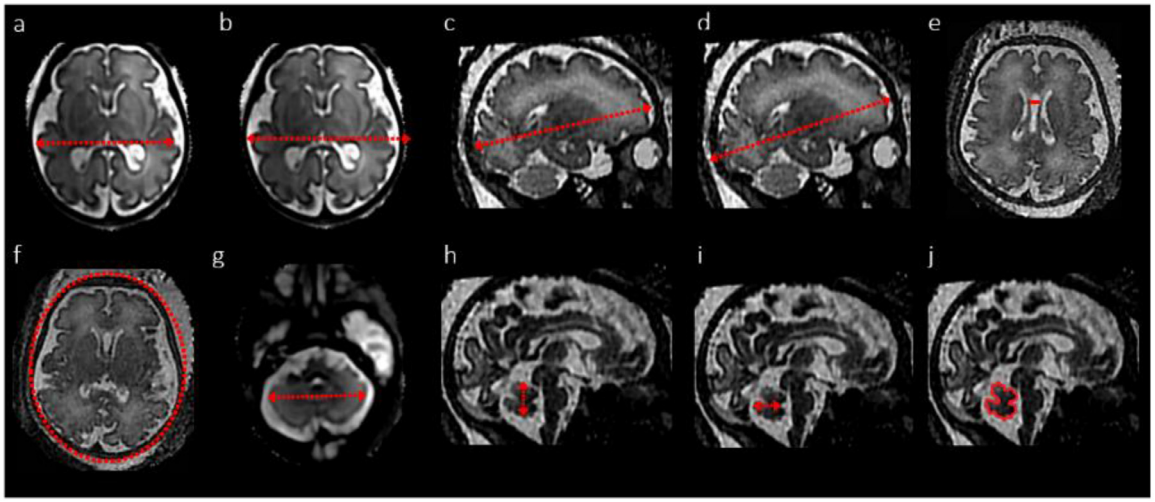

Fig. 1. Visual representation of linear measurements in the fetal brain in the axial plane (a: BPD–brain, (b): BPD–skull, (c): OFD–brain, (d): OFD–skull, (e): cavum width, (f): HC, (g): TCD; (h): vermis height; (i): vermis width; (j): vermis surface area).

confirm appropriate appearance for gestation. Image datasets showing an overt additional malformation were excluded. All T2-weighted images were reviewed to assess image quality and those with excessive motion, which could not be automatically accurately segmented, were excluded. As such, three fetal cases were excluded as they could not be reconstructed due to image quality and severe motion artefacts.

Image analysis

Linear measurements

Fetal and neonatal brain linear measurements were performed on reconstructed images using ImageJ (version 1.46R, National Institutes of Health, Bethesda, MD, USA), and based on the following parameters (Kyriakopoulou et al., 2017; Salomon et al., 2010). Fig. 1; (a) Biparietal diameter (BPD) brain–maximum brain width in the transverse plane, outermost to outermost edge; (b) Biparietal diameter (BPD) skull–the widest diameter of the fetal skull measured in the transverse plane, outermost to innermost edge; (c) Occipitofrontal diameter (OFD) brain–the maximum distance of the brain width between the frontal and occipital lobes, measured in the sagittal plane, outermost to outermost edge; (d) Occipitofrontal diameter (OFD) skull–the maximum distance between the frontal and occipital skull bones, measured in the sagittal plane, outermost to innermost edge (e) Cavum width–largest width in the transverse plane; (f) Head circumference (HC)–calculated using the equation: head circumference = –1.62 x [(skull BPD) + (skull OFD)]; (g) Transcerebellar diameter (TCD)–the maximum lateral cerebellar distance in the transverse plane. All vermis measurements were taken in the mid-sagittal plane, (h) Vermis height–the maximum superior-inferior length; (i) Vermis width–the maximum distance between the fastigium and the posterior part of the vermis; and (j) Vermis area–calculated using a free hand drawing tool.

Fetal volumetric segmentation

Volumetric segmentation of the supratentorial brain tissue, lateral ventricles and extra-cerebral CSF (eCSF) was performed in a semi-automated manner, whilst the cortex and cerebellum were manually segmented using ITK-SNAP (Yushkevich et al., 2006) using the following parameters; (a) Supratentorial brain tissue volume–brain tissue above the tentorium, excluding the brainstem, cerebellum and any CSF spaces; (b) Cortical volume–total cerebral cortical grey matter; (c) Total ventricular volume–combined volumes of the left and right ventricles, including the choroid plexus, but excluding the third and fourth ventricle, the cavum septum pellucidum and cavum vergae (CSP); (d) eCSF volumes–all the intracranial CSF spaces surrounding the supratentorial brain tissue and cerebellum and including the interhemispheric fissure but not any ventricular structure, the CSP or vergae; and (e) Total cerebellar volume–both cerebellar hemispheres and the vermis and excluding the pons and fourth ventricle (Fig. 2a-e). To ensure compatibility between volumetric data acquired from 1.5T and 3T reconstructions, a healthy pregnant volunteer was scanned on both scanners on the same day. Volumetric data were compared and no significant differences were found between the two images across any of the key fetal brain segmentation regions; volumes were within the excepted +/− 5% threshold.

Neonatal volumetric segmentation

T2-weighted images were segmented using *The Developing Brain Region Annotation With Expectation-Maximization (Draw-EM)* MIRTK Package, a fully automated tissue segmentation algorithm, optimised for the neonatal brain (Makropoulos et al., 2014). Tissue segmentations were visually inspected for accuracy and any mislabelled voxels were manually edited using ITK–SNAP. Volumetric analysis was performed on supratentorial brain tissue, cortical, cerebellar, eCSF and lateral ventricular volumes. Supratentorial brain tissue volumes were calculated by the sum of cortical grey matter, deep grey matter and white matter volumes (Fig. 3).

Statistical analysis

Statistical analysis was performed using the SPSS software package (SPSS Chicago, IL, USA; version 24) and MATLAB (Release: 2017a, The MathWorks, Inc., Natick, MA, USA), and visualised using GraphPad Prism (GraphPad software, La Jolla, CA, USA; version 8.00). Each variable was tested for normality, non-normally distributed data were log-transformed. Linear and volumetric measurements for the combined fetal and neonatal cohorts were analysed using nested random effects in a fit random intercept linear mixed-effects model (LME) to compare results between the two groups (DS and controls), controlling for the covariate GA/PMA as a fixed effect, and with a subject dependent random effect for the intercept to account for repeated measures. GA/PMA is a continuous variable throughout our analyses. Cohen's *d* values were obtained to assess effect sizes and the magnitude of interactions (Cohen, 1988; Rosenthal and Rosnow, 2008). Effect sizes were interpreted as small (Cohen's *d*value $\leq$ 0.4), medium (0.5–0.7) and large ($\geq$ 0.8) (Cohen, 1988). A post-hoc False Discovery Rate (FDR) test

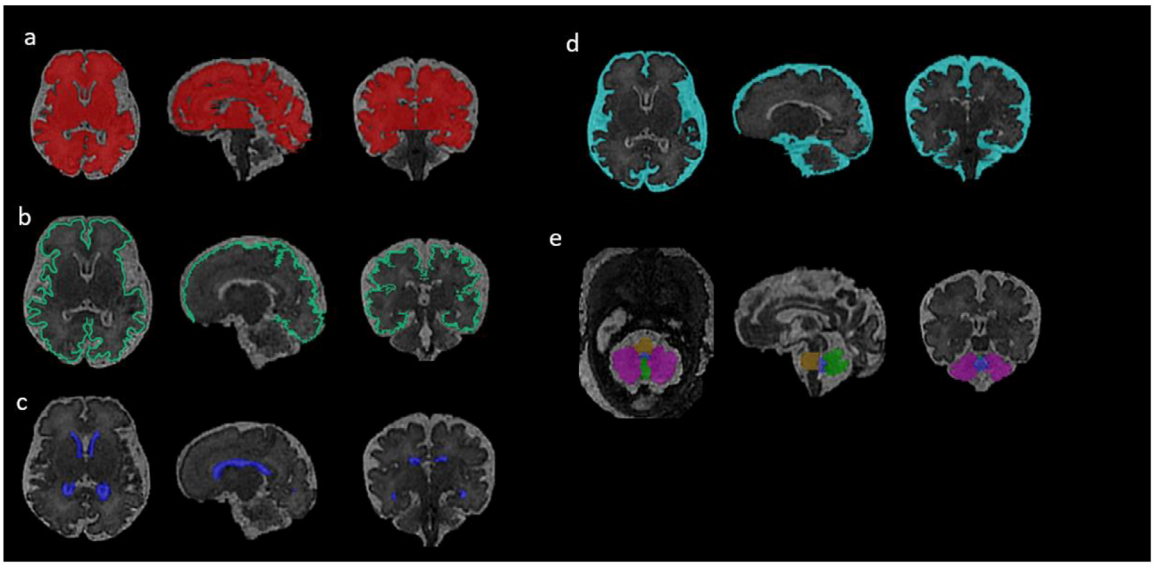

Fig. 2. Volumetric segmentation of the fetal brain. Segmentation of T2-weighted volumetric MR images in the axial, sagittal and coronal planes showing (a) supratentorial brain tissue (red), (b) cortex (green), (c) lateral ventricles (dark blue), (d) extra cerebral cerebrospinal fluid (light blue); and (e) cerebellar hemispheres (pink), cerebellar vermis (bright green), pons (yellow) and fourth ventricle (blue).

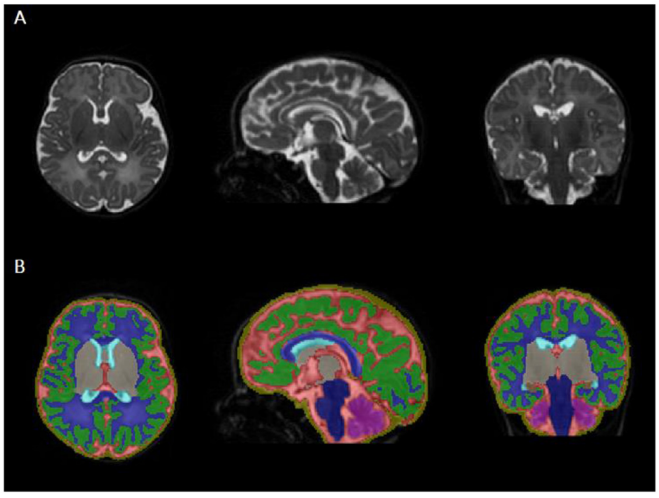

Fig. 3. Volumetric segmentation of the neonatal brain. (a) Reconstructed T2 neonatal brain, (b) automatic neonatal brain segmentation; supratentorial brain tissue (bright blue + green + gray), cortex (green), lateral ventricles (light blue), extra cerebral cerebrospinal fluid (red), cerebellar hemispheres (pink); and brainstem (deep blue).

was performed for multiple comparisons, using the Benjamini-Hochberg (1995) procedure (Benjamini and Hochberg, 1995), controlling the alpha error to 5%. Correlations were assessed using the Pearson's correlation coefficient (Pearson's r) on normally distributed data and the Spearman's correlation coefficient (Spearman's r) on non-normally distributed data.

All image analysts (PP, VK, AD and EA) were required to perform linear measurements and volumetric analyses in a sub-cohort of ten fetuses. Cases were selected to span the gestational period studied (GA 21.71, 22.86, 25.29, 26.14, 28.29, 29.57, 31.71, 32.71, 34, and 36 weeks). All results were checked and verified by the most experienced observers. The inter-rater and intra-rater variability was assessed for each region of interest and the threshold for differences was set at +/− 5%. If concordance was not reached, the analyses was repeated across all regions of interest until all results were within the 5% threshold. Observers were not blinded to cases as control cases had previously been analysed.

Results

Control cohort

A total of 52 control fetuses (GA at scan: mean (range)–29.58 (22.43–38.86) weeks), and 21 control neonates (PMA at scan: mean (range) 41.58 (38–46) weeks) were included as part of this study (Table 1). The control neonatal cohort was comprised of 11 male and 10 female participants. We were unable to obtain the sex ratio for the control fetal cohort, as sex was not documented at the time of scan.

DS cohort

30 fetuses with DS, of which 17 fetuses with cardiac defects (GA at scan: mean (range)–29.28 (21.86–35.71) weeks) and 13 without cardiac defects (GA at scan: mean (range)–30.82 (22.14–35.43) weeks) were included in the study. Six fetuses (GA range at scan: 21.86–35.71 weeks) were scanned again as neonates (PMA range at scan: 39.00–44.57).

21 neonates with DS were scanned; 16 with cardiac defects (PMA at scan: mean (range)–40.51 (36–46) weeks) and 5 without cardiac defects (PMA at scan: mean (range)–42.20 (39–44) weeks). Of these 21 DS neonates, 11 were born at term (GA at birth: 37–41.71 weeks) and imaged between 37.57–45.57 weeks PMA; the other 10 neonates were born prematurely (GA at birth: 31.43–36.71 weeks) and scanned between 32.43–44.57 weeks PMA (Table 1).

The DS cohort was comprised of 21 male and 23 female participants

Table 1
Combined fetal and neonatal DS and control cohorts, pre and post 28 weeks' gestational age (GA); post-menstrual age (PMA).

	Control GA < 28 weeks	DS GA > 28 weeks	GA < 28 weeks	GA > 28 weeks
Total number	$N = 21$	$N = 52$	$N = 10$	$N = 41$
GA/PMA range (weeks)	22.43–27.57	28–45	21.86–27.14	28.14–46
Mean GA/PMA at scan (weeks)	25.07	36.05	25.22	36.71

Table 2
Summary of the DS cohort, with and without a congenital heart defect (CHD).

	DS Cardiac abnormalities(DS + CHD)	Non-cardiac (DS–CHD)
Total number	$N = 33$	$N = 18$
GA/PMA range (weeks)	21.86–46	22.14–44
Mean GA/PMA at scan (weeks)	34.72	33.98

(Supplementary Table 1). The first line of analysis aimed to compare regional brain volumes between the DS cohort and the controls during the second trimester (GA < 28 weeks), and in the combined third trimester and neonatal period (GA > 28 weeks) (Table 1). As 10 of our neonates were born prematurely and scanned shortly after birth, and therefore not at term equivalent age, we felt it was appropriate to include these in our grouped analysis alongside third trimester fetuses. Secondary analysis was performed to investigate the effect of a CHD on regional brain volumes in the DS cohort–cohorts were examined as a whole across gestation and postnatally and not subdivided by trimester (Table 2).

Results are presented by region of interest, starting with whole brain and cortical measures, followed by cerebellar findings and finally CSF measures.

Whole brain and cortical development

All volumetric and linear brain and skull measures were positively correlated with increasing GA (Fig 3). Fetuses and neonates with DS were found to have significantly smaller whole brain volumes in the second and third trimester, and postnatally (supratentorial brain tissue ($p < 0.001$, $d = 1.64/1.74$); Table 3 & 4, Fig. 4a). However, cortical volumes only started to deviate from the normal cohort in the third trimester ($p < 0.001$), after 28 weeks GA (Table 3, Fig. 4b). No differences in whole brain or cortical volumes were found between the DS fetuses and neonates with a congenital cardiac defect (DS + CHD) and those without (DS–CHD).

Fetuses and neonates with DS had significantly smaller brain OFD ($p < 0.001$, Fig 4f), in the second and third trimester compared to age matched controls. Skull OFD ($p < 0.001$, Fig 4e) and HC ($p < 0.001$, Fig 4g) were only found to be significantly smaller in the third trimester, from 28 weeks GA (Table 3; Fig. 4). Skull and brain BPD were not significantly different between the two cohorts at any time point. There were no significant differences in 2D linear measurements between the DS fetuses with and without cardiac abnormalities (Table 4). No significant differences were found in whole brain and cortical measures between DS males and females when corrected for multiple comparisons.

Cerebellum

2D and volumetric cerebellar measurements in the DS cohort were significantly smaller than in the control population; cerebellar volume ($p < 0.001$), transcerebellar diameter (TCD) ($p < 0.001$), vermis height, width and surface area ($p < 0.001$) (Table 3; Fig. 5). Cerebellar volumes, vermis height and surface area were consistently smaller in the DS cohort, during the second trimester. The TCD and vermis width, however, were only smaller in the DS cohorts from the third trimester. We observed large effect sizes across all cerebellar measures throughout the third trimester and postnatally (Table 3). Cerebellar volumes in late gestation DS fetuses and neonates were disproportionately smaller with respect to whole brain volumes, compared to the control population. These group differences remained significant when cerebellar volumes were corrected for cortical volume and head circumference. No

Table 3
LME results and Cohen's *d* values for 2D and 3D brain measures comparing the control *vs* DS cohort: * = significant result, $p < 0.05$. Biparietal diameter (BPD), Occipitofrontal diameter (OFD), Head Circumference (HC), and Transcerebellar diameter (TCD), Effect sizes interpreted as small (Cohen's $d = \leq 0.4$), medium (0.5–0.7) and large (≥ 0.8).

Volumetric/Linear measurements	Estimate		Standard Error		df		*t* value		*p* value		Cohen's d	
	GA < 28 weeks	GA > 28 weeks	GA < 28 weeks	GA > 28 weeks	GA < 28 weeks	GA > 28 weeks	GA < 28 weeks	GA > 28 weeks	GA < 28 weeks	GA > 28 weeks	GA < 28 weeks	GA > 28 weeks
Whole brain and cortex												
Whole brain (cm3)	19.06	53.02	4.48	6.40	27	91	4.25	8.29	< 0.001	< 0.001	1.64	1.74
Cortex (cm3)	0.75	17.41	1.06	3.93	27	91	0.71	4.42	0.54	< 0.001	0.27	0.93
BPD Skull (mm)	−0.65	0.80	1.49	0.88	27	91	-0.44	0.90	0.69	0.44	−0.17	0.19
BPD Brain (mm)	2.63	1.30	1.21	0.81	27	91	2.17	1.61	0.06	0.14	0.83	0.34
OFD Skull (mm)	2.46	4.72	1.35	1.02	27	91	1.83	4.64	0.11	< 0.001	0.70	0.97
OFD Brain (mm)	4.67	6.81	1.28	1.03	27	91	3.65	6.63	< 0.001	< 0.001	1.40	1.39
HC (mm)	2.92	8.95	4.27	2.68	27	91	0.68	3.33	0.54	< 0.001	0.26	0.70
Cerebellum												
Cerebellum (cm3)	0.58	4.99	0.21	0.51	27	91	2.77	9.84	0.02	< 0.001	1.06	2.06
TCD (mm)	1.12	2.22	0.65	0.45	27	91	1.73	4.91	0.12	< 0.001	0.67	1.03
Vermis height (mm)	2.66	3.41	0.36	0.39	27	91	7.36	8.73	0.00	< 0.001	2.83	1.83
Vermis width (mm)	0.60	1.67	0.38	0.36	27	91	1.59	4.59	0.15	< 0.001	0.61	0.96
Vermis surface area (mm2)	29.90	67.58	5.12	8.15	27	91	5.84	8.30	0.00	< 0.001	2.25	1.74
CSF spaces												
Lateral Ventricles (cm3)	−4.46	−3.12	1.49	0.56	27	91	-2.99	-5.55	0.02	< 0.001	−1.15	−1.16
eCSF (cm3)	0.21	3.04	3.29	3.74	27	91	0.06	0.81	0.95	0.48	0.02	0.17
Cavum width (mm)	0.89	−0.97	0.45	0.45	26	72	1.97	−2.14	0.09	0.06	0.77	−0.51

Table 4
LME results and Cohen's *d* values for 2D and 3D measures comparing the DS − CHD *vs* DS + CHD cohort: *= significant result, $p < 0.05$. Biparietal diameter (BPD), Occipitofrontal diameter (OFD), Head Circumference (HC), and Transcerebellar diameter (TCD). Effect sizes interpreted as very small (Cohen's $d = 0.01$), small (0.20), medium (0.50); large (0.80); very large (1.20); and huge (2.0).

DS-CHD compared to DS + CHD Volumetric/Linear measurements	Estimate	Standard Error	df	*t* value	*p* value	Cohen's d
Whole brain and cortex						
Whole brain (cm3)	13.89	8.75	48	1.59	0.28	0.46
Cortex (cm3)	0.39	6.11	48	0.06	0.95	0.02
BPD Skull (mm)	3.42	1.52	48	2.25	0.20	0.65
BPD Brain (mm)	3.08	1.49	48	2.07	0.20	0.60
OFD Skull (mm)	2.49	1.77	48	1.41	0.28	0.41
OFD Brain (mm)	2.74	1.80	48	1.52	0.28	0.44
HC (mm)	9.53	4.84	48	1.97	0.23	0.57
Cerebellum						
Cerebellum (cm3)	0.57	0.63	48	0.90	0.50	0.26
TCD (mm)	0.68	0.72	48	0.95	0.50	0.27
Vermis height (mm)	0.23	0.59	48	0.39	0.70	0.11
Vermis width (mm)	0.96	0.58	48	1.64	0.28	0.47
Vermis surface area (mm2)	5.91	12.61	48	0.47	0.76	0.14
CSF spaces						
Lateral Ventricles (cm3)	3.24	1.31	48	2.48	0.20	0.72
eCSF (cm3)	7.65	5.53	48	1.38	0.28	0.40
Cavum width (mm)	−0.25	0.66	34	−0.38	0.76	−0.13

differences in cerebellar measures were found in the DS cohort with a CHD, compared to those without a CHD (Table 4). Visually, there appear to be differences in the overall growth trajectories between DS + CHD compared to DS–CHD, however these were not found to be statistically significant. No significant differences were found in cerebellar measures between DS males and females when corrected for multiple comparisons.

Cerebrospinal fluid (CSF) regions

Lateral ventricular volumes were larger in DS cases compared to controls throughout the second and third trimester, with a large observed effect size ($p < 0.001$, $d = -1.5/-1.6$; Table 3, Fig 6a). Extra cerebral CSF (eCSF; Fig 6b) volumes and cavum pellucidum width were not significantly different ($p > 0.05$) (Table 3, Fig. 6). No significant differences were found in those DS cases with a CHD, compared to those without. Additionally, no significant differences were found in CSF measures between DS males and females when corrected for multiple comparisons.

We ran an additional analysis comparing volumetric and linear measures from DS fetal patients acquired on the 1.5T ($n = 12$) and 3T ($n = 18$) scanners and found no statistically significant differences, when corrected for GA.

Discussion

Using state-of-the-art *in vivo* MR imaging, we have identified quantifiable alterations from 21 weeks' gestation in brain development of fetuses and neonates with DS. This study highlights growth trajectories of specific brain structures in the developing DS brain, and more importantly the varying time points during gestation when deviations arise. We found early second trimester deviations in whole brain and cerebellar volumes, and subsequent third trimester alterations in cortical and ventricular volumes, and in overall head circumferences. Despite the noted group-wise differences in brain development (DS compared to age-matched controls), we found overlap in almost all assessed parameters, highlighting a spectrum of atypical development across the DS cohort. This is of interest but perhaps not unexpected given the recognised individual variability in neurodevelopmental outcome of DS individuals, as established for instance, by IQ scores (Karmiloff-Smith et al., 2016; Turner and Alborz, 2003; Carr, 1988; Startin et al., 2016).

This study used *in vivo* MRI to detect early deviations in cerebellar and cortical growth during DS fetal and subsequently neonatal development. We observed large effect sizes associated with global decreases in whole brain and cortical volumes in the DS population. A recent proof-of-principle study also observed deviations from 28 weeks GA, which we have confirmed in a larger cohort (Tarui et al., 2019). Decreased brain and cerebellar growth between 24 and 40 weeks GA are likely biological substrates for impaired neurocognitive abilities in later childhood, especially complex functions relating to planning and attention (Rathbone et al., 2011). Reductions in brain size and altered cellular configurations, such as aberrant cortical lamination, reduction in dendritic ramifications and diminished synaptic formation (Becker et al., 1986) have all been detected postmortem in DS. More specifically, human postmortem morphometric and ultrastructural studies have shown a 20–50% reduction in neurons (from birth until 14 years of age), in the granular layers of the cerebral cortex along with an abnormal distribution of neurons in cortical layers II and IV (Schmidt-Sidor et al., 1990, Wisniewski, 1990; Wisniewski et al., 1984). In addition, studies that assessed dendritic morphology and arborisation in PM tissue have found that newborns and older infants with DS had shorter dendrites, a reduction in the number of spines and altered neuronal morphology ($n = 7$; 26 weeks GA–11 months) whilst DS fetuses exhibited the same neuronal morphology and dendritic spines as control fetuses (Takashima et al., 1981). It is, therefore, likely that the anatomical volumetric reductions demonstrated with *in vivo* MRI reflect the changes in the underlying neurobiology. Decreasing growth trajectories over time, could be indicative of detrimental reductions in neuronal proliferation and migration, alterations in dendrite morphology and impaired cortical connectivity with increasing age, or even cell death. MRI provides an excellent and safe *in vivo* assessment to monitor these changes across gestation and postnatally.

Our study also found reduced cerebellar volumes in the DS cohort, with more marked deviations from aged-matched controls arising with increasing PMA. This supports findings from previous MRI studies on fetal, infant, child, adolescent and adult DS populations where decreased cerebellar volumes were reported (Tarui et al., 2019; Aylward et al., 1997; White et al., 2003; Haydar and Reeves, 2012; Levman et al., 2019; Shiohama et al., 2019). Cerebellar volumetric abnormalities, have previously been associated with cognitive functions such as impaired attention, language, abstract reasoning, attention, working memory and executive control (Strick et al., 2009; Menghini et al., 2011). Neurodevelopmental assessments have demonstrated that children with DS performed worse than the typically developing children in the spatial-simultaneous working memory tasks, attributable to variations in cortical and cerebellar growth (Lanfranchi et al., 2014). Mouse models of DS have implicated the gene Dyrk1A in specific structural and functional cerebellar phenotypes, including reduced volume (García-Cerro et al., 2014). Cerebellar neurons are mainly formed prenatally, with some granule cell layer formation postnatally (Bartesaghi et al., 2011). Human postmortem fetal studies have found evidence of impaired cellular formation, in the form of hypocellularity in the DS cerebellum which are the likely underlying cause of the gross volume reduction on MRI (Guidi et al., 2011, Baburamani et al., 2019).

TCD measures were found to be reduced in the DS cohort, with a statistically significant reduction in the third trimester and postnatally. Smaller TCD measures, acquired from US imaging, have previously been reported in DS fetuses (Reddy et al., 2017). We also observed large effect sizes associated with decreased cerebellar volumes, which are consistent with reduced TCD results. In addition, reductions in 2D linear measurements of vermian height, width and surface area were

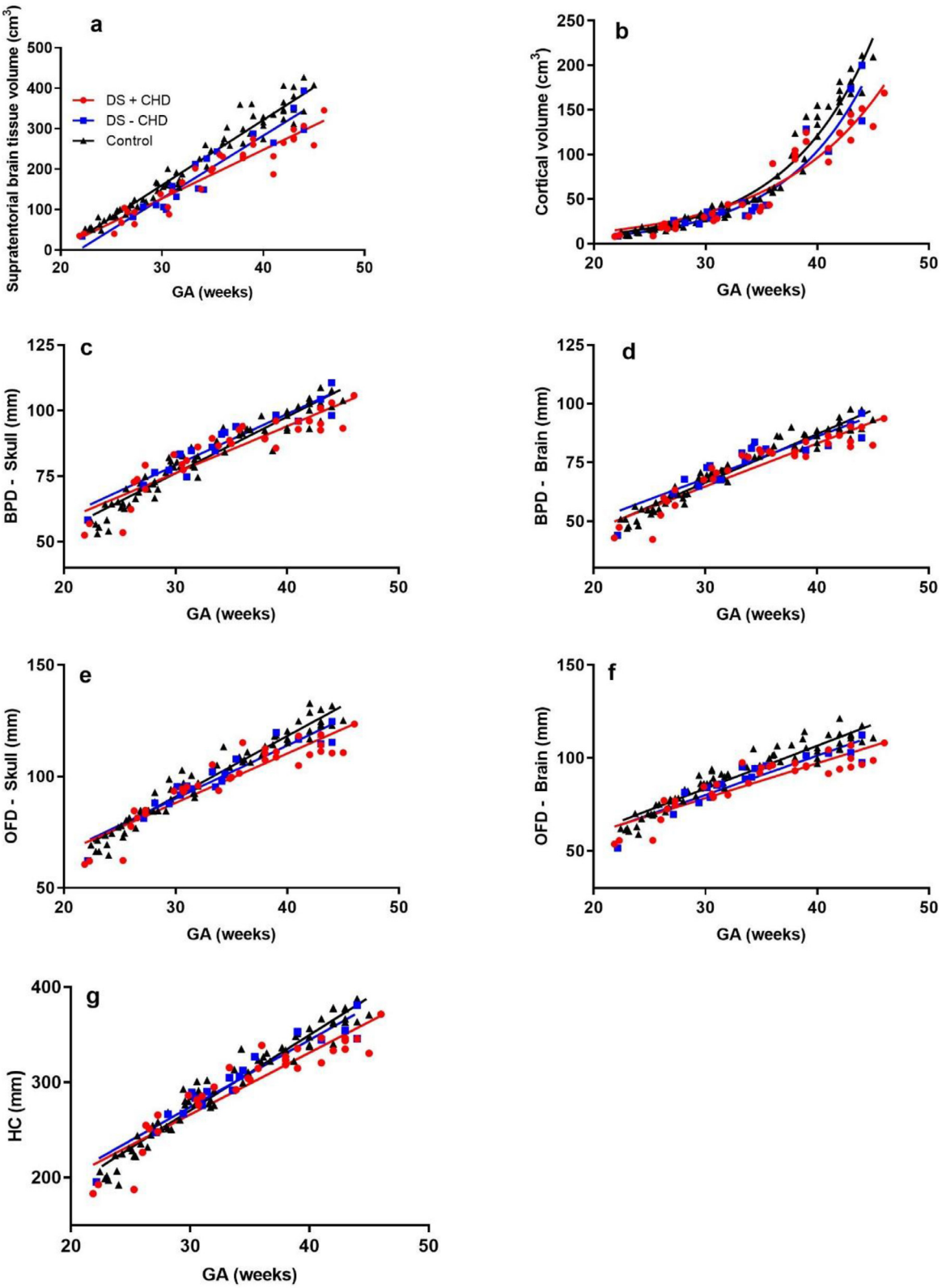

Fig. 4. 2D and 3D regional measures of the brain in fetuses and neonates with DS and a congenital heart defect (DS + CHD; red circles), DS without a congenital heart defect (DS–CHD; Blue squares), and age-matched normal controls (black triangles). (a) Whole brain volumes, (b) Cortical volumes, (c) Biparietal diameter (BPD)–skull, (d) Biparietal diameter (BPD)–brain, (e) Occipitofrontal diameter (OFD)–skull, (f) Occipitofrontal diameter (OFD)–brain, and (g) Head circumference (HC) (MRI derived).

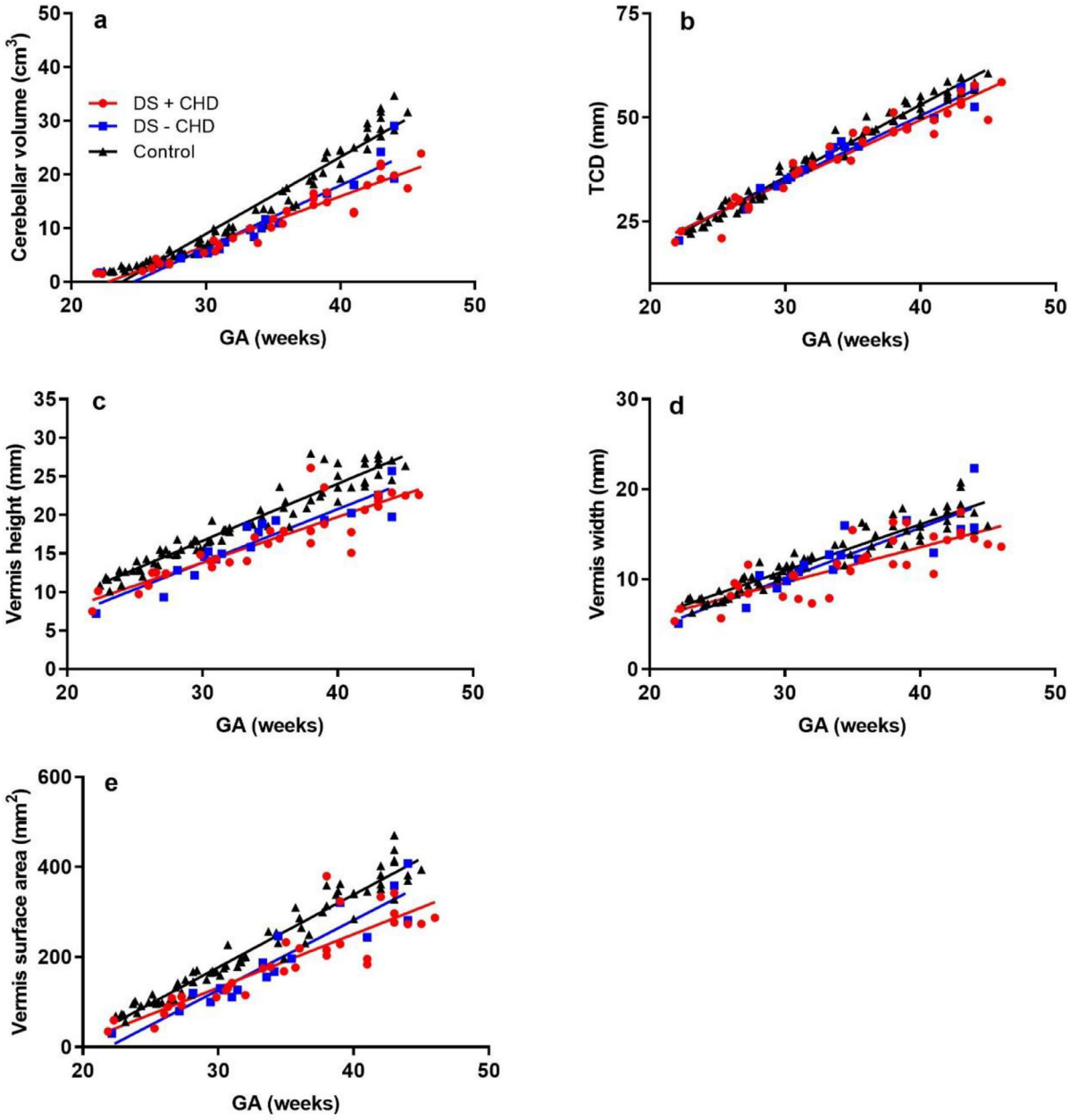

Fig. 5. 2D and 3D measures of the cerebellum in fetuses and neonates with DS and a congenital heart defect (DS + CHD; red circles), DS without a congenital heart defect (DS–CHD; blue squares), and age-matched normal controls (black triangles). (a) Cerebellar volume, (b) Transcerebellar diameter, (c) Vermis height (d) Vermis width, and (e) Vermis surface area.

seen in the DS cerebellum compared with controls from 21 weeks GA. Whilst not conventionally performed in clinical practice, the fetal cerebellar vermis has successfully been measured on US (Cignini et al., 2016; Spinelli et al., 2016), and it is possible that additional vermis height measures during the fetal anomaly US scan might increase the non-invasive detection of fetuses with DS at an earlier time point.

We identified reduced 2D brain and skull parameters from as early as the second trimester, in addition to an altered ratio of OFD to BPD, which is consistent with previous reports of DS populations having a brachycephalic skull. The brachycephalic skull reflects a similarly shaped brain and is considered to be a consequence of relatively smaller frontal lobes in DS (Pinter and Eliez, 2001). Frontal lobe dysfunction and structural changes have previously been associated with early manifestations of Alzheimer's disease in the adult DS population (Dykens, 2007; Fonseca et al., 2016). Further analysis of regional brain volumes in early postnatal development will allow us to explore the relationship between frontal lobe development and childhood cognitive abilities. However, we emphasize that our data is preliminary, and we are not in a position to make any concrete links between results presented here and data obtained on adult patients with Alzheimer's disease.

The DS cohort had significant lateral ventricular enlargement at both the fetal and neonatal time points, compared to controls, as indicated by a large effect size. However, eCSF volumes were similar between groups across gestation. Previous DS fetal US studies have reported enlargement of the lateral ventricles (Schimmel et al., 2006). Isolated fetal ventriculomegaly in non-DS children has been associated with mild cognitive impairment (Beeghly et al., 2010). Lateral ventricular dilation is known to increase across the lifespan and is reflective of atrophy of surrounding brain tissue; this is particularly prominent in adults with Alzheimer's Disease pathology (Koran et al., 2014). Early ventricular enlargement is, however, likely to be developmental in

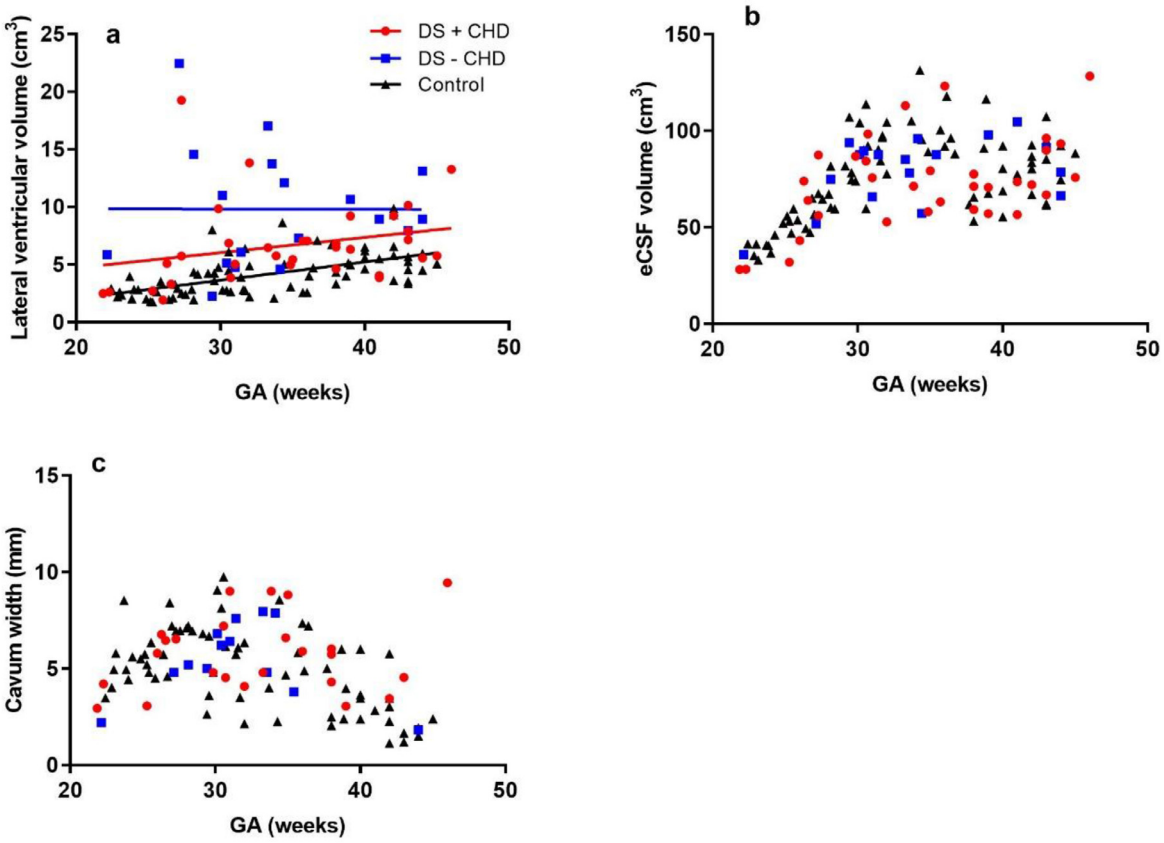

Fig. 6. 2D and 3D measures of the CSF regions in fetuses and neonates with DS and a congenital heart defect (DS + CHD; red circles), DS without a congenital heart defect (DS – CHD; blue squares), and age-matched normal controls (black triangles). (a) Lateral ventricular volume, (b) eCSF volume, and (c) Cavum width.

origin. DS murine models have demonstrated that overexpression of the calmodulin regulator protein, Purkinje cell protein 4 (Pcp4), contributes to impaired ciliary function in ependymal cells and results in brain ventriculomegaly (Raveau et al., 2017).

Whilst we hypothesised that regional brain volumes would be significantly smaller in the DS cohort with a cardiac defect, we did not find statistically significant differences (following correction for multiple comparisons) between the DS cohorts with or without a CHD. Abnormalities in brain development of fetuses with CHD, have reported increased incidences of ventriculomegaly, without evidence of an underlying chromosomal abnormality, (Khalil et al., 2016; Brossard-Racine et al., 2014; Mebius et al., 2017). Our study did not find a statistically significant elevation in lateral ventricular volume, despite observing a medium effect size. However, when assessing the graphs visually it is evident that a number of cases with increased ventricular volumes, are in DS cases without a CHD. Other studies in neonates with CHD have focused on atypical growth and development of the cortex, which has been attributed to alterations in cerebral blood flow and oxygenation and the presence of transposition of the great arteries (TGA) and hypoplastic left heart (Kelly et al., 2017). The cardiac conditions in our cohort with DS were primarily endocardial cushion defects such as AVSD, where antenatal changes in blood flow and oxygenation are less prominent than in TGA (Peyvandi and Donofrio, 2018). Previous studies have reported a poorer outcome in individuals with DS who have an associated CHD (Visootsak et al., 2011; Visootsak et al., 2013; Visootsak et al., 2016). More detailed studies of the postnatal brain development in DS with and without a cardiac defect may be enlightening, as it is possible that the specific genes responsible for a cardiac abnormality in DS may have an additional direct effect on brain development (Lana-Elola et al., 2016).

The primary limitation of this study is the small sample size of the DS cohort to date. DS pregnancy termination statistics were 90% in 2012, as reported by the National Down Syndrome Cytogenetic Register in England and Wales (Morris and Springett, 2014). The live-birth rate of DS has remained relatively stable over the last 30 years (Wu and Morris, 2013), consequently we found recruitment to be challenging. In addition, we combined images from a 1.5T and a 3T scanner for fetal imaging (all neonates were imaged on a 3T scanner). Images acquired from scanners with a stronger magnetic field and higher quality optimised receiver coils, benefit from an increased signal to noise ratio (SNR), consequently there may be differences in the acquired resolution and contrast of the resultant reconstruction. Previous studies found that while most of the brain was identically classified at the two field strengths, there were some regional differences observed (West et al., 2013). Others have reported highly reproducible volumetric data in adults with AD and controls, scanned on 1.5T and 3T scanners (Roche et al., 2013). Upon closer investigation when comparing DS fetal datasets acquired on 1.5T (n = 12) and 3T (n = 18) scanners, we were able to conclude that there were no discernible differences in volumetric data.

We segmented the cortex in all of our cases, but were not able to delineate the subplate consistently. The subplate is a transitional structure which varies across gestational age and progressively merges with the underlying white matter as gyrification progresses; unlike the cortex which has a contrasting signal and is seen in its entirety at all gestations. Whilst we appreciate the biological and developmental importance of the subplate we could not accurately assess its volume with our current approach. This however would be of interest for future studies.

In conclusion, this study has demonstrated alterations in both cortical and cerebellar development detectable by *in vivo* MR imaging *in utero* from the second trimester. Individuals with DS are now living to

middle age, with improved quality of life and decreases in early mortality as a consequence of medical interventions, and improved surgical repair of CHDs (Wu and Morris, 2013; Jensen and Bulova, 2014; Glasson et al., 2002). The majority of individuals with DS, however, demonstrate cognitive decline in early adulthood. Strategies to modify this decline are already taking place (Livingstone et al., 2015; Gardiner, 2015, De la Torre et al., 2014) with researchers also testing therapeutic interventions to improve early brain development which may in turn decrease the likelihood of subsequent declines (Stagni et al., 2015). Later neurodevelopmental assessments in our cohort will allow us to determine whether deviations in these antenatal indices are predictive of severity of subsequent cognitive impairments in DS and thereby may provide a suitable *in vivo* tool to assess future interventions.

CRediT authorship contribution statement

Prachi A. Patkee: Data curation, Formal analysis, Investigation, Methodology, Project administration, Software, Validation, Visualization, Writing - original draft, Writing - review & editing. **Ana A. Baburamani:** Funding acquisition, Investigation, Project administration, Validation, Writing - review & editing. **Vanessa Kyriakopoulou:** Data curation, Formal analysis, Investigation, Methodology, Validation, Writing - review & editing. **Alice Davidson:** Data curation, Formal analysis, Methodology, Validation. **Elhaam Avini:** Formal analysis, Funding acquisition, Validation. **Ralica Dimitrova:** Data curation, Investigation, Writing - review & editing. **Joanna Allsop:** Data curation, Investigation, Methodology. **Emer Hughes:** Data curation, Investigation, Methodology. **Johanna Kangas:** Data curation, Investigation. **Grainne McAlonan:** Conceptualization, Funding acquisition, Investigation, Methodology, Project administration, Supervision, Writing - review & editing. **Mary A. Rutherford:** Conceptualization, Funding acquisition, Investigation, Methodology, Project administration, Supervision, Validation, Writing - review & editing.

Declaration of competing interest

The authors declare that they have no competing interests.

Acknowledgements

We thank the parents and children who participated in this study. The authors gratefully acknowledge staff from the Center for the Developing Brain at King's College London and the Neonatal Intensive Care Unit at St. Thomas' Hospital. In particular, the research radiologists, radiographers, clinicians, neonatal nurses, midwives and the administrative teams. In addition, we wish to thank all our obstetric and fetal medicine colleagues from our patient identification sites who have referred participants to us.

This work was supported by the Medical Research Council [MR/K006355/1 and MR/LO11530/1]; Rosetrees Trust [A1563], Fondation Jérôme Lejeune [2017b–1707], Sparks and Great Ormond Street Hospital Children's Charity [V5318] . We also gratefully acknowledge financial support from the Wellcome/EPSRC Center for Medical Engineering [WT 203148/Z/16/Z] , the National Institute for Health Research (NIHR) Biomedical Research Center (BRC) based at Guy's and St Thomas' NHS Foundation Trustand King's College London and supported by the NIHR Clinical Research Facility (CRF) at Guy's and St Thomas'. The Brain Imaging in Babies (BIBS) team additionally acknowledge support from EU-AIMS– a European Innovative Medicines Initiative; and infrastructure support from the National Institute for Health Research (NIHR) Mental Health Biomedical Research Center (BRC) at South London and Maudsley NHS Foundation Trust and King's College London.

The views expressed are those of the author(s) and not necessarily those of the NHS, the NIHR or the Department of Health.

Supplementary materials

Supplementary material associated with this article can be found, in the online version, at doi:10.1016/j.nicl.2019.102139.

References

Holtzman, D., ... 1996. The human trisomy 21 brain: insights from mouse models of Down syndrome. Ment. Retard. 72, 66–72.
Antonarakis, S.E., Lyle, R., Dermitzakis, E.T., Reymond, A., Deutsch, S, 2004. Chromosome 21 and down syndrome: from genomics to pathophysiology. Nat. Rev. Genet. 5, 725–738.
Määttä, T., Tervo-Määttä, T., Taanila, A., Kaski, M., Iivanainen, M, 2006. Mental health, behaviour and intellectual abilities of people with Down syndrome. Down Syndr. Res. Pract. 11, 37–43.
Rachidi, M., Lopes, C., 2007. Mental retardation in Down syndrome: from gene dosage imbalance to molecular and cellular mechanisms. Neurosci. Res. 59, 349–369.
Bartesaghi, R., Guidi, S., Ciani, E., 2011. Is it possible to improve neurodevelopmental abnormalities in Down syndrome. Rev. Neurosci. 22, 419–455.
Karmiloff-Smith, A, et al., 2016. The importance of understanding individual differences in Down syndrome. F1000Res. 5, 389.
Hyett, J., Noble, P., Snijders, R., Montenegro, N., Nicolaides, K., 1996. Fetal heart rate in trisomy 21 and other chromosomal abnormalities at 10–14 weeks of gestation. Ultrasound Obstet. Gynecol. 7, 239–244.
Roizen, N.J., Patterson, D, 2003. Down's syndrome. Lancet 361, 1281–1289.
Sherman, S., Allen, E.E.G., Bean, L.H., Freeman, S.B., 2007. Epidemiology of Down syndrome. Ment. Retard. Dev. Disabil 13, 221–227.
Bergstrom, S, et al., 2016. Trends in congenital heart defects in infants with Down syndrome. Pediatrics 138, 1–9.
Razzaghi, H., Oster, M., Reefhuis, J., 2015. Long term outcomes in children with congenital heart disease: national health interview survey. J. Pediatr. 166, 119–124.
Visootsak, J, et al., 2011. Neurodevelopmental outcomes in children with Down syndrome and congenital heart defects. Am. J. Med. Genet. A 155A, 2688–2691.
Visootsak, J., Hess, B., Bakeman, R., Adamson, L.B., 2013. Effect of congenital heart defects on language development in toddlers with Down syndrome. J. Intellect. Disabil. Res. 57, 887–892.
Visootsak, J, et al., 2016. Influence of CHDs on psycho-social and neurodevelopmental outcomes in children with Down syndrome. Cardiol. Young 26, 250–256.
Rachidi, M., Lopes, C, 2011. Mental retardation and human chromosome 21 gene overdosage : from functional genomics and molecular mechanisms towards prevention and treatment of the neuropathogenesis of Down syndrome. In: Genomics, Proteomics and the Nervous system, pp. 21–86. https://doi.org/10.1007/978-1-4419-7197-5.
Guedj, F, et al., 2016. An integrated human/murine transcriptome and pathway approach to identify prenatal treatments for Down syndrome. Sci. Rep. 6, 32353.
Hamner, T., Udhnani, M.D., Osipowicz, K.Z., Lee, N.R., 2018. Pediatric brain development in Down syndrome: a field in its infancy. J. Int. Neuropsychol. Soc. 1–11. https://doi.org/10.1017/S1355617718000206.
Borenstein, M., Dagklis, T., Csapo, B., Sotiriadis, A., Nicolaides, K.H., 2006. Brachycephaly and frontal lobe hypoplasia in fetuses with trisomy 21 at 11 + 0 to 13 + 6 weeks. Ultrasound Obstet. Gynecol. 28, 870–875.
Winter, T., Ostrovsky, A., Komarniski, C., Uhrich, S., 2000. Cerebellar and frontal lobe hypoplasia in fetuses with Trisomy 21: usefulness as combined US markers 1. Radiology 533–538.
Jiang, S, et al., 2007. MRI of moving subjects using multislice snapshot images with volume reconstruction adult brain studies. IEE Trans. Med. Imaging 26, 967–980.
Kuklisova-Murgasova, M., Quaghebeur, G., Rutherford, M.a, Hajnal, J.V., Schnabel, J.a., 2012. Reconstruction of fetal brain MRI with intensity matching and complete outlier removal. Med. Image Anal. 16, 1550–1564.
Yushkevich, P.A., et al., 2006. User-guided 3D active contour segmentation of anatomical structures: significantly improved efficiency and reliability. Neuroimage 31, 1116–1128.
Kyriakopoulou, V, et al., 2017. Normative biometry of the fetal brain using magnetic resonance imaging. Brain Struct. Funct. 222, 2295–2307.
Hughes, E.J, et al., 2017. A dedicated neonatal brain imaging system. Magn. Reson. Med. 78, 794–804.
Salomon, L.J, et al., 2010. GUIDELINES practice guidelines for performance of the routine mid-trimester fetal ultrasound scan. Ultrasound Obs. Gynecol. https://doi.org/10.1002/uog.8831.
Makropoulos, A, et al., 2014. Automatic whole brain MRI segmentation of the developing neonatal brain. IEEE Trans. Med. Imaging 33, 1818–1831.
Cohen, J., 1988. Statistical Power Analysis For the Behavioral sciences. Lawrence Earlbaum Associates.
Rosenthal, R., Rosnow, R., 2008. Essentials of Behavioral Research: Methods and Data Analysis. McGraw-Hill.
Benjamini, Y., Hochberg, Y., 1995. Controlling the false discovery rate: a practical and powerful approach to multiple. J Royal Statist. Soc. 57.
Turner, S., Alborz, A., 2003. Academic attainments of children with Down's syndrome: a longitudinal study. Br. J. Educ. Psychol. 73, 563–583.
Carr, J, 1988. Six weeks to twenty-one years old: a longitudinal study of children with DS and their families. J. Child Psychol. Psychiatry 29, 407–431.

Startin, C.M, et al., 2016. The LonDownS adult cognitive assessment to study cognitive abilities and decline in Down syndrome. Wellcome open Res. 1, 11.
Tarui, T, et al., 2019. Quantitative MRI analyses of regional brain growth in living fetuses with Down syndrome. Cereb. Cortex 00, 1–9.
Rathbone, R, et al., 2011. Perinatal cortical growth and childhood neurocognitive abilities. Neurology 77, 1510–1517.
Becker, L.E., Armstrong, D.L., Chan, F., 1986. Dendritic atrophy in children with Down's syndrome. Ann. Neurol. 20, 520–526.
Schmidt-Sidor, B., Wisniewski, K., Shepard, T., Sersen, E., 1990. Brain growth in Down syndrome subjects 15–22 weeks gestational age and birth to 60 months. Clin. Neuropathol. 9.
Wisniewski, K., 1990. Down syndrome children often have brain with maturation delay, retardation of growth, and cortical dysgenesis. Am. J. Med. Genet. Suppl. 7.
Wisniewski, K., Laure-Kamionowska, M., Wisniewski, H., 1984. Evidence of arrest of neurogenesis and synaptogenesis in brains of patients with Down Syndrome. N. Engl. J. Med. 311, 1187–1188.
Takashima, S., Becker, L.E., Armstrong, D.L., Chan, F.-.W., 1981. Abnormal neuronal development in the visual cortex of the human fetus and infant and down's syndrome. Brain Res. 225, 1–21.
Aylward, E.H, et al., 1997. Cerebellar volume in adults with Down syndrome. Arch. Neurol. 54, 209–212.
White, N.S., Alkire, M.T., Haier, R.J., 2003. A voxel-based morphometric study of nondemented adults with Down syndrome. Neuroimage 20, 393–403.
Haydar, T.F., Reeves, R.H, 2012. Trisomy 21 and early brain development. Trends Neurosci. 35, 81–91.
Levman, J., et al., 2019. Structural magnetic resonance imaging demonstrates abnormal cortical thickness in Down syndrome: newborns to young adults. NeuroImage Clin. 23.
Shiohama, T., Levman, J., Baumer, N., Takahashi, E., 2019. Structural magnetic resonance imaging-based brain morphology study in infants and toddlers with Down syndrome: the effect of comorbidities. Pediatr. Neurol. https://doi.org/10.1016/j.pediatrneurol.2019.03.015.
Strick, P.L., Dum, R.P., Fiez, J.A, 2009. Cerebellum and nonmotor function. Annu. Rev. Neurosci. 32, 413–434.
Menghini, D., Costanzo, F., Vicari, S., 2011. Relationship between brain and cognitive processes in Down syndrome. Behav. Genet. 41, 381–393.
Lanfranchi, S., Mammarella, I.C., Carretti, B., 2014. Spatial-simultaneous working memory and selective interference in Down syndrome. Child Neuropsychol. 1–9. https://doi.org/10.1080/09297049.2014.913557.
García-Cerro, S., et al., 2014. Overexpression of Dyrk1A is implicated in several cognitive, electrophysiological and neuromorphological alterations found in a mouse model of Down syndrome. PLoS ONE 9, e106572.
Guidi, S., Ciani, E., Bonasoni, P., Santini, D., Bartesaghi, R., 2011. Widespread proliferation impairment and hypocellularity in the cerebellum of fetuses with down syndrome. Brain Pathol. 21, 361–373.
Baburamani, A.A., Patkee, P.A., Arichi, T., Rutherford, M.A., 2019. New approaches to studying early brain development in Down syndrome. Dev. Med. Child Neurol. 1–13. https://doi.org/10.1111/dmcn.14260.
Reddy, R.H., Prashanth, K., Ajit, M., 2017. Significance of foetal transcerebellar diameter in foetal biometry: a pilot study. J. Clin. Diagnostic Res. 11, TC01–TC04.
Cignini, P., et al., 2016. Reference charts for fetal cerebellar vermis height: a prospective cross-sectional study of 10605 fetuses. PLoS ONE 11, 1–20.
Spinelli, M., et al., 2016. Fetal cerebellar vermis circumference measured by 2-Dimensional ultrasound scan: reference range, feasibility and reproducibility. Ultrasound Int. Open 02, E124–E128.
Pinter, J., Eliez, S., ... 2001. Neuroanatomy of Down's syndrome: a high-resolution MRI study. Am. J. 1659–1665.
Dykens, E., ... 2007. Psychiatric and behavioral disorders in persons with Down syndrome. Ment. Retard. Dev. Disabil. 13, 272–278.
Fonseca, L.M., Yokomizo, J.E., Bottino, C.M., Fuentes, D., 2016. Frontal lobe degeneration in adults with dDown syndrome and Alzheimer's disease: a review. Dement. Geriatr. Cogn. Disord. 41, 123–136.
Schimmel, M.S.M., Hammerman, C., Bromiker, R., Berger, I., 2006. Third ventricle enlargement among newborn infants with trisomy 21. Pediatrics 117, e928–e931.
Beeghly, M, et al., 2010. Neurodevelopmental outcome of fetuses referred for ventriculomegaly. Ultrasound Obstet. Gynecol. 35, 405–416.
Koran, M.E.I, et al., 2014. Differences in age-related effects on brain volume in Down syndrome as compared to Williams syndrome and typical development. J. Neurodev. Disord. 6, 8.
Raveau, M, et al., 2017. Brain ventriculomegaly in Down syndrome mice is caused by Pcp4 dose-dependent cilia dysfunction. Hum. Mol. Genet. 26, 923–931.
Khalil, A., et al., 2016. Prevalence of prenatal brain abnormalities in fetuses with congenital heart disease: a systematic review. Ultrasound Obstet. Gynecol. 48, 296–307.
Brossard-Racine, M, et al., 2014. Prevalence and spectrum of in utero structural brain abnormalities in fetuses with complex congenital heart disease. Am. J. Neuroradiol. 35, 1593–1599.
Mebius, M., Kooi, E., Bilardo, C., Bos, A., 2017. Brain injury and neurodevelopmental outcome in congenital heart disease: a systematic review. Pediatrics 140, e20164055.
Kelly, C.J, et al., 2017. Impaired development of the cerebral cortex in infants with congenital heart disease is correlated to reduced cerebral oxygen delivery. Sci. Rep. 7, 1–10.
Peyvandi, S., Donofrio, M., 2018. Circulatory changes and cerebral blood flow and oxygenation during transition in newborns with congenital heart disease. Semin. Pediatr. Neurol. https://doi.org/10.1016/j.spen.2018.05.005.
Lana-Elola, E, et al., 2016. Genetic dissection of Down syndrome-associated congenital heart defects using a new mouse mapping panel. Elife 5, 1–20.
Morris, J.K., Springett, A., 2014. The national Down syndrome cytogenetic register for England and Wales. 2012 Annual Report 44, 0–31.
Wu, J., Morris, J.K., 2013. The population prevalence of Down's syndrome in England and Wales in 2011. Eur. J. Hum. Genet. 21, 1033–1034.
West, J., Blystad, I., Engström, M., Warntjes, J.B.M., Lundberg, P., 2013. Application of quantitative MRI for brain tissue segmentation at 1.5 T and 3.0 T field strengths. PLoS ONE 8, 1–12.
Roche, F., et al., 2013. Reproducibility of intracranial and hippocampal volume quantification at 1.5T and 3T MRI: application to ADNI I. Alzheimer's Dement. 9, P271.
Jensen, K.M., Bulova, P.D., 2014. Managing the care of adults with Down's syndrome. BMJ. https://doi.org/10.1136/bmj.g5596.
Glasson, E., et al., 2002. The changing survival profile of people with Down's syndrome: implications for genetic counselling. Clin. Genet. 62, 390–393.
Livingstone, N., Hanratty, J., Mcshane, R., Macdonald, G., 2015. Pharmacological interventions for cognitive decline in people with Down syndrome (Review). Cochrane Database Syst. Rev doi:10.1002/14651858.CD011546.pub2.www.cochranelibrary.com.
Gardiner, K.J., 2015. Pharmacological approaches to improving cognitive function in Down syndrome : current status and considerations. Drug Des. Devel. Ther 9, 103–125.
De la Torre, R., et al., 2014. Epigallocatechin-3-gallate, a DYRK1A inhibitor, rescues cognitive deficits in Down syndrome mouse models and in humans. Mol. Nutr. Food Res 58, 278–288.
Stagni, F., Giacomini, A., Guidi, S., Ciani, E., Bartesaghi, R., 2015. Timing of therapies for Down syndrome: the sooner, the better. Front. Behav. Neurosci. 9, 265.